A New Superconducting Oxycarbonitrate: $(Tl_{5/6}Cr_{1/6})Sr_4Cu_2(CO_3)_{1/2}(NO_3)_{1/2}O_7$

A. Barnabé, F. Letouzé, D. Pelloquin,* A. Maignan, M. Hervieu, and B. Raveau

Laboratoire CRISMAT, ISMRA et Université de Caen, UMR 6508 associée au CNRS Bd du Maréchal Juin, 14050 Caen Cedex, France

Received May 16, 1997. Revised Manuscript Received July 29, 1997[⊗]

The introduction of nitrate groups in the derivatives of the Tl "1201" structure is shown for the first time. A new superconducting oxycarbonitrate $(Tl_{5/6}Cr_{1/6})Sr_4(CO_3)_{1/2}(NO_3)_{1/2}O_7$ is isolated. It crystallizes in a tetragonal cell with $a = 3.8320(1)$ Å and $c = 16.4112(5)$ Å and a P-type lattice. This compound contains, like the superconducting oxycarbonate $(Tl_{2/3}Cr_{1/3})Sr_4Cu_2(CO_3)O_7$, hexavalent chromium, but it differs fundamentally from the latter by its structure. The $(Tl_{5/6}Cr_{1/6})Sr_4Cu_2(CO_3)_{1/2}(NO_3)_{1/2}O_7$ structure consists of a single intergrowth of the "1201" and S_2CC ($Sr_2CuO_2CO_3$) structures, whereas $(Tl_{2/3}Cr_{1/3})Sr_4Cu_2(CO_3)O_7$ is a (110)-sheared structure derived from the latter by a shearing mechanism every five CuO_6 octahedra. The transition between the two structures is discussed in terms of a size mismatch between Cr and Tl species. The critical temperature of the oxycarbonitrate is close to 65 K. The relations of this new compound with the 77 K superconducting oxycarbonate $(Tl_{2/3}Cr_{1/3})Sr_4Cu_2(CO_3)O_7$ and the 34 K superconducting oxychromate $Tl_3(CrO_4)Sr_8Cu_4O_{16}$ are discussed.

Introduction

A large series of thallium and mercury superconducting oxycarbonates has been synthesized to date. All these compounds exhibit the generic formula $(Tl,M)_1A_4Cu_2CO_3O_7$ or $(Hg,M)_1A_4Cu_2CO_3O_{6-\delta}$, where A is Ba and/or Sr and M is a transition or a posttransition element (see for a review refs 1 and 2). Despite their identical compositions, three different forms of oxycarbonates must be distinguished, named single intergrowth, (100)-sheared, and (110)-sheared, respectively. The first form, $(1201)_1(S_2CC)_1$, corresponds to the intergrowth of the "1201" structure, e.g., $(Tl,M)_1Sr_2CuO_5$ or $(Hg,M)_1Sr_2CuO_{4-\delta}$ with the S_2CC structure ($Sr_2CuO_2CO_3$), whereas the two other forms derive from the simple intergrowth $(1201)_1(S_2CC)_1$ by a shearing mechanism transversally to the copper layers, along the (100) and the (110) planes, respectively.

Although numerous compounds have been synthesized, the factors that determine the stability of one form rather than another one are not known to date. For instance the single intergrowth oxycarbonates are only obtained for pure "Sr_4" strontium phases, whereas most of the (100) or (110)-sheared oxycarbonates require the presence of barium and strontium simultaneously. Nevertheless the mixed "$Sr_{4-x}Ba_x$" presence is not an imperative condition for the stabilization of the sheared phases, since pure strontium compounds such as $(Tl_{4/5}V_{1/5})Sr_4Cu_2CO_3O_7$ and $(Tl_{2/3}Cr_{1/3})Sr_4Cu_2CO_3O_7$[3] exhibit a (110)-sheared structure. The difficulty to determine the different factors responsible for the shearing phenomena comes from the fact that two kinds of sites may be involved, the Tl or Hg sites and the Sr(Ba) sites (a M for Cu substitution could also be considered, depending on the M nature). Moreover, the three forms are rarely observed in the same system, so that it is difficult to draw conclusions. The system $Hg_{1-x}V_xSr_{4-y}Ba_yCu_2CO_3O_{6-\delta}$ is, to date, the only one that exhibits the three crystallographic forms.[4−5] The fact that the single intergrowth corresponds to the low Ba content ($y < 1.8$) whereas the sheared structures are obtained for $y > 1.8$ suggests that the Ba/Sr ratio is an important parameter. Nevertheless, it also clearly appears that the Hg/V ratio varies ($0.28 \leq \times \leq 0.4$), so that this factor may also play a role in the stabilization of the different forms.

As pointed out above, the synthesis of the 77 K superconductor $(Tl_{2/3}Cr_{1/3})Sr_4Cu_2(CO_3)O_7$ is of interest since it is one of the rare pure "Sr_4" oxycarbonates that exhibits a sheared structure. For this reason, we have attempted to vary in this compound the Tl/Cr ratio keeping the "Sr_4" content fixed, to detect the possible transition to a second form. Such an investigation could be carried out by replacing partly the CO_3 groups by NO_3 groups that exhibit an almost identical geometry. We report herein on a superconductor $Tl_{5/6}Cr_{1/6}Sr_4(CO_3)_{1/2}(NO_3)_{1/2}O_7$, single intergrowth-type structure.

Experimental Procedure

In a first step, the system $Tl_{1-x}Cr_xSr_4Cu_2(CO_3)_{3x}(NO_3)_{1-3x}O_7$ was investigated starting from various mixtures of the oxides $(1-x)/2Tl_2O_3$, $x/2Cr_2O_3$, $3xSrCO_3$, $(1-3x)/2Sr(NO_3)_2$, $1CuO$, $3/2(1-x)SrO_2$, and $1Sr_2CuO_3$. After different attempts, it was observed that the nitrate groups tend to be partly decomposed during the reaction so that they substitute with difficulty for carbonate groups. Thus an excess of nitrate (yNO_3) is necessary to manage the syntheses according to the ratio $(1-x)/2Tl_2O_3$, $x/2Cr_2O_3$, $3xSrCO_3$, $(1-3x+y)/2Sr(NO_3)_2$, $1CuO$, (3

[⊗] Abstract published in *Advance ACS Abstracts,* September 15, 1997.

(1) Raveau, B.; Hervieu, M.; Michel, C. *Physica C* **1996**, *263*, 151.
(2) Raveau, B.; Michel, C.; Mercey, B.; Hamet, J. F.; Hervieu, M. *J. Alloys Compounds* **1995**, *229*, 134.
(3) Maignan, A.; Pelloquin, D.; Malo, S.; Michel, C.; Hervieu, M.; Raveau, B. *Physica C* **1995**, *249*, 220.
(4) Malo, S.; Pelloquin, D.; Maignan, A.; Michel, C.; Hervieu, M.; Raveau, B. *Physica C* **1996**, *269*, 1.
(5) Hervieu, M.; Pelloquin, D.; Malo, S.; Michel, C.; Raveau, B. *J. Solid State Chem.* **1996**, *126*, 271.

S0897-4756(97)00370-0 CCC: $14.00

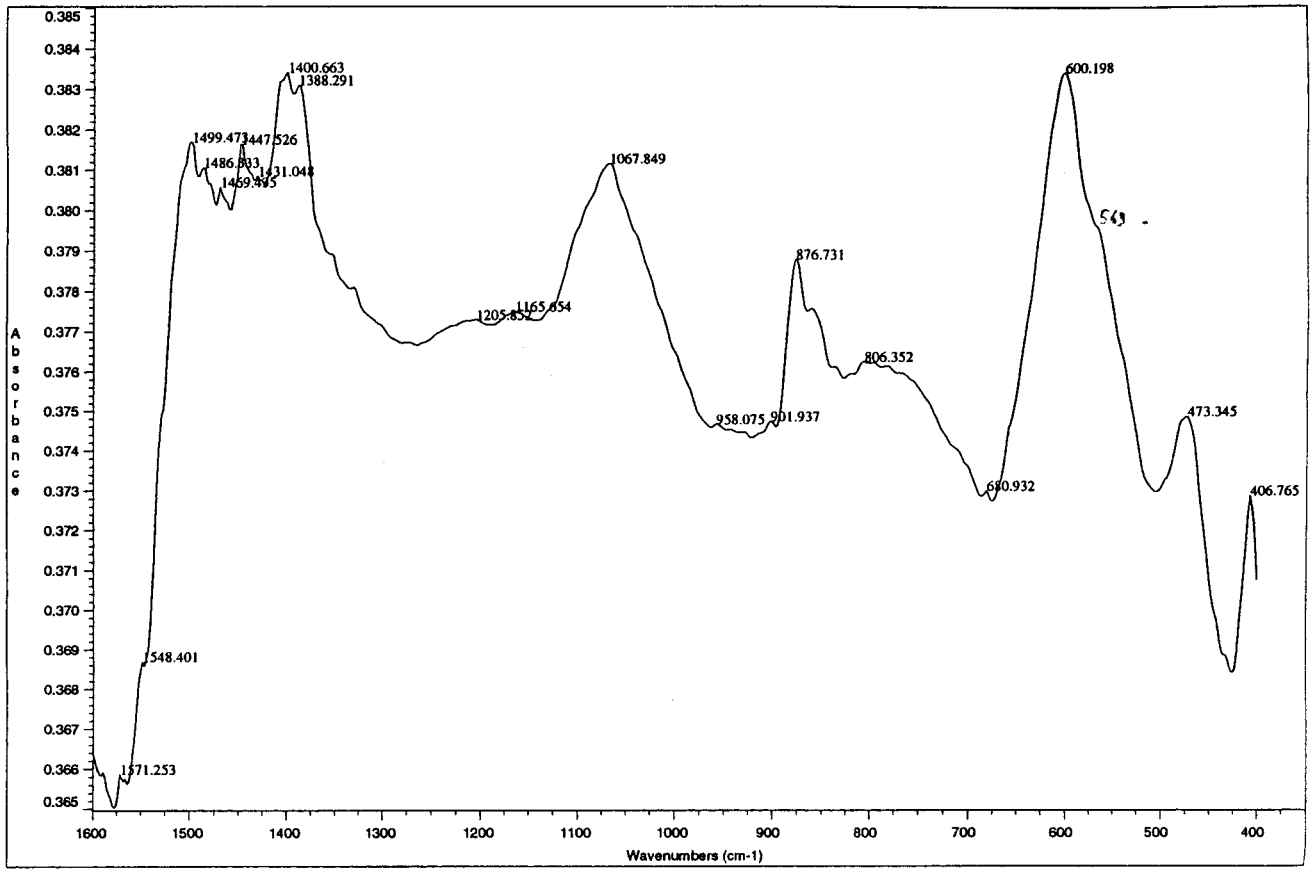

Figure 1. $Tl_{5/6}Cr_{1/6}Sr_4Cu_2(CO_3)_{1/2}(NO_3)_{1/2}O_7$: infrared spectrum.

$- 3x - y)/2SrO_2$, and $1Sr_2CuO_3$. The precursors were then weighed according to the chosen nominal $[x, y]$ composition, intimately ground in an agate mortar, pressed in the form of bars, and placed in an alumina finger. Next, the mixture was sealed in an evacuated silica ampule before applying the following thermal treatment: the compounds were directly introduced in the hot furnace at 850 °C, kept at this temperature for 15 h, and quenched down to room temperature.

The electron diffraction (ED) study was carried out using a JEOL 200 CX electron microscope fitted with an eucentric goniometer (±60°) and equipped with an EDX analyzer. The high-resolution electron microscopy (HREM) was performed with a TOPCON 002B operating at 200 KV and having a point resolution of 1.8 Å. HREM images calculations were carried out with the Mac Tempas multislice program.

The powder X-ray diffraction (XRD) data were collected with a Philips vertical diffractometer (Cu Kα radiation) in the range $6° \leq 2\theta \leq 110°$ by increment of 0.02° (2θ).

The ac susceptibility measurements were measured between 4 and 300 K with an AC Lakeshore susceptometer. No demagnetization corrections were applied, due to the porous character of the ceramics.

Results and Discussion

Exploring the above nominal range $Tl_{1-x}Cr_xSr_4Cu_2(CO_3)_{3x}(NO_3)_{1-3x+y}O_{7\pm\delta}$, for $0 \leq \times \leq {}^1/_3$ and $0 \leq y \leq 1$, a new phase is obtained for $x \approx 0.17$ and $y \approx 0.5$.

The EDS analysis performed on many microcrystals shows that the cation ratio is close to the nominal one, i.e., "$Tl_{5/6}Cr_{1/6}Sr_4Cu_2$". The infrared spectrum shows three bands at 1400−1500, 1067, and 876 cm^{-1} (Figure 1). They can be attributed to the presence of CO_3^{2-}, NO_3^-, and CrO_4^{2-} groups, respectively. The latter observation is of great interest since it confirms the presence of nitrate groups and shows that chromium is present in the form of the chromate group, i.e., is hexavalent and exhibits a tetrahedral coordination; from the IR data, there is no evidence of the presence of Cr at a lower oxidation state. This hexavalent oxidation state of chromium in an oxidizing atmosphere was expected, taking into consideration the parent "1201" oxychromate $Tl_3(CrO_4)Sr_8Cu_4O_{16}$,[6-7] whose neutron diffraction study shows that Cr(VI) is definitely involved in the form of CrO_4 tetrahedra. Consequently, the ideal formula $Tl_{5/6}Cr_{1/6}Sr_4Cu_2(CO_3)_{1/2}(NO_3)_{1/2}O_7$ can be proposed for the new phase.

The reconstruction of the reciprocal space, using electron diffraction evidenced a tetragonal cell, with $a \approx a_p$ and $c \approx 16.4$ Å (a_p is the parameter of the cubic perovskite cell). There is no condition limiting the reflections. The [001], [$\bar{1}$10] and [010] ED patterns are displayed in Figure 2.

The cell parameters were refined from powder X-ray diffraction data to $a = 3.831(1)$ Å, $c = 16.4112(5)$ Å, with the possible space groups $P4$, $P4/m$, $P422$, $P4mm$, $P\bar{4}2m$, $P4/mmm$, and $P\bar{4}m2$. Although the diffractogram is close to the (110)-sheared oxycarbonate $(Tl_{2/3}Cr_{1/3})Sr_4Cu_2CO_3O_7$,[3] the cell parameters of this new phase show a great difference since the latter compound is orthorhombic with $a = 5.418$ Å $= a_p\sqrt{2}$, $b = 5a_p\sqrt{2} = 27.108$ Å, and $c = 16.668$ Å. The value of the c parameter, significantly smaller than that of $(Tl_{2/3}Cr_{1/3})Sr_4Cu_2(CO_3)O_7$, suggests that the structure of $Tl_{5/6}Cr_{1/6}Sr_4Cu_2(CO_3)_{1/2}(NO_3)_{1/2}O_7$ is not sheared.

(6) Martin, C.; Letouzé, F.; Maignan, A.; Seshadri, R.; Michel, C.; Hervieu, M.; Raveau, B. *Chem. Mater.* **1996**, *8*, 865.

(7) Michel, C.; Letouzé, F.; Martin, C.; Hervieu, M.; Raveau, B. *Physica C* **1996**, *262*, 159.

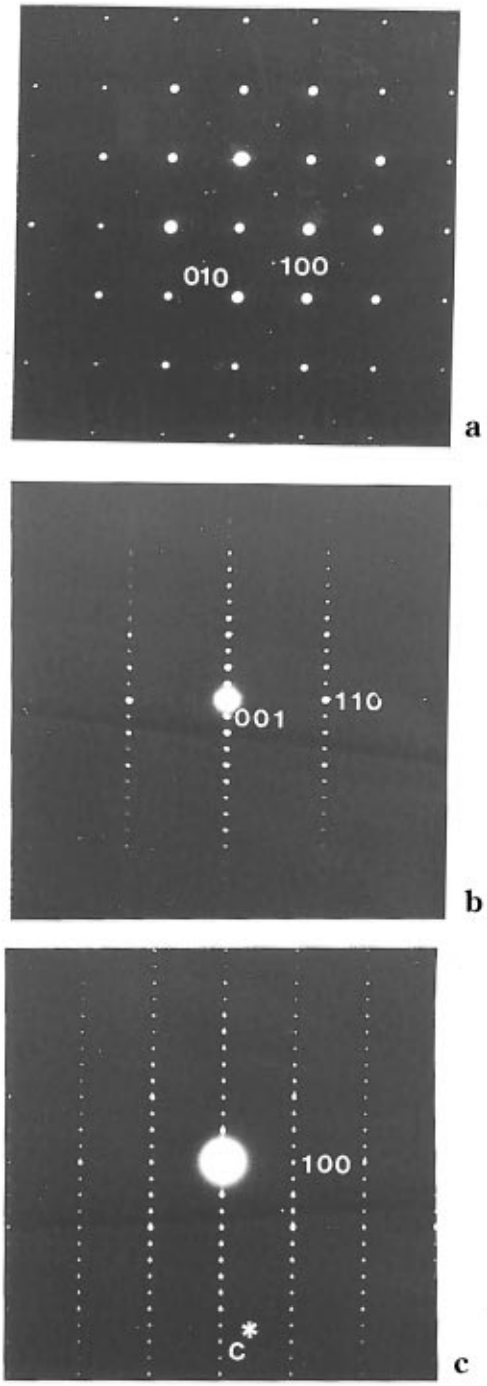

Figure 2. (a) [001], (b) [$\bar{1}$10], and (c) [010] ED patterns.

The high-resolution electron microscopy (HREM) study confirmed the above hypothesis. The contrast can be easily interpreted referring to the experimental and simulated images previously reported for other oxycarbonates.[1−5,8−10] The stacking of the copper and carbonitrate layers along *c* is highly regular as shown from the [110] HREM image displayed in Figure 3a. For this focus value, the mixed carbonate−nitrate layers are imaged as rows of very bright dots and the copper layer octahedra as rows of gray dots. The two types of layers

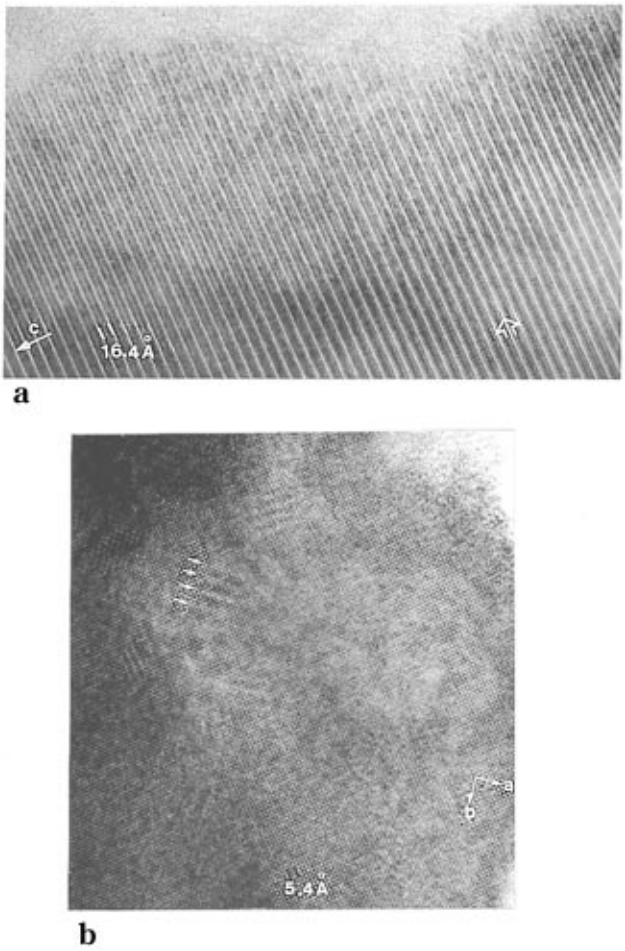

Figure 3. (a) [110] and (b) [001] HREM images. In (a) the carbonate layers appear as rows of bright dots (one of them is indicated by a white arrow).

Table 1. Refined Structural Parameters for $(Tl_{5/6}Cr_{1/6})Sr_4Cu_2(CO_3)_{1/2}(NO_3)_{1/2}O_7$

atom	site	*x*	*y*	*z*	*B* (Å)	*n*
Tl	1a	0.102(2)	0	0	0.7(2)	0.85(1)
Cr	1a	0.102(2)	0	0	0.7(2)	0.15(1)
Sr(1)	2h	0.5	0.5	0.1592(2)	1.3(1)	2
Sr(2)	2h	0.5	0.5	0.3723(2)	1.6(1)	2
Cu	2g	0	0	0.2630(3)	1.1(1)	1
C / N	1b	0	0	0.5	1	1
O(1)	1c	0.5	0.5	0	1	1
O(2)	2g	0	0	0.1226(12)	1	2
O(3)	8s	0.141(8)	0	0.4306(12)	1	2
O(4)	4m	0.332(8)	0	0.5	1	1
O(5)	4i	0.5	0	0.2719(8)	1	4

space group	*P*4/*mmm*
lattice parameters	$a = 3.83201(8)$ Å, $c = 16.4112(5)$ Å
reliability factors	$R_p = 0.067$, $R_{WP} = 0.086$, $R_B = 0.052$, $\chi^2 = 2.41\%$

alternate very regularly. The [001] images consist of regular arrays of white dots, which are spaced 2.8 Å along the [110] and [$\bar{1}$10] directions (Figure 3b). This is in agreement with the tetragonal cell with $a \approx a_p$.

The refinement of the structure from the powder XRD data corroborates the HREM observations, leading to a final R_B factor close to 0.05 for the positional parameters listed in Tables1 and 2.

The structure of the oxycarbonitrate $(Tl_{5/6}Cr_{1/6})$-$Sr_4Cu_2(CO_3)_{1/2}(NO_3)_{1/2}O_7$ (Figure 4a) consists of a single intergrowth of one "1201"-type layer, formulated $[Tl_{5/6}Cr_{1/6}Sr_2CuO_5]$, with one S_2CC-type layer, which would be formulated $[Sr_2CuO_2(CO_3)_{1/2}(NO_3)_{1/2}]$. The

(8) Hervieu, M.; Michel, C.; Huvé, M.; Martin, C.; Maignan, A.; Raveau, B. *Microsc. Microanal. Microstruct.* **1993**, *1*, 1.
(9) Milat, O.; Van Tendeloo, G.; Amelinckx, S.; Babu, T. G. N.; Greaves, C. *J. Solid State Chem.* **1994**, *109*, 5.
(10) Zhang, X. F.; Van Tendeloo, G.; Amelinckx, S.; Pelloquin, D.; Michel, C.; Hervieu, M.; Raveau, B. *J. Solid State Chem.* **1994**, *113*, 2,327.

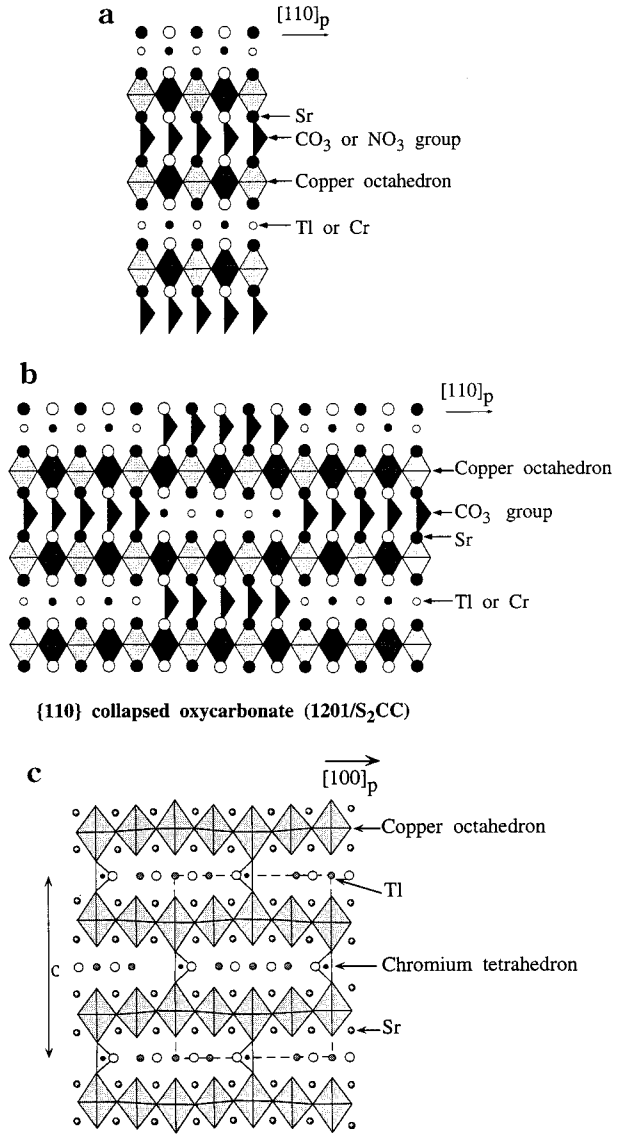

Figure 4. Idealized structures of (a) the simple intergrowth $(Tl_{5/6}Cr_{1/6})Sr_4Cu_2(CO_3)_{1/2}(NO_3)_{1/2}O_7$ (b) the (110)-sheared oxycarbonate $(Tl_{2/3}Cr_{1/3})Sr_4Cu_2CO_3O_7$ and (c) the ordered 1201 oxychromate $Tl_3(CrO_4)Sr_8Cu_4O_{16}$.

Table 2. Selected Interatomic Distances (Å) and Angles (deg)

Tl/Cr−O(1) × 2 = 2.448(5)	Cu−O(2) × 1 = 2.31(2)
Tl/Cr−O(2) × 2 = 2.05(2)	Cu−O(3) × 1 = 2.80(2)
	Cu−O(5) × 4 = 1.922(1)
Sr(1)−O(1) × 1 = 2.612(3)	
Sr(1)−O(2) × 4 = 2.775(5)	C/N−O(3) × 1 = 1.26(2)
Sr(1)−O(5) × 4 = 2.664(9)	C/N−O(4) × 2 = 1.27(1)
Sr(2)−O(3) × 2 = 2.55(2)	O(3)−C−O(4) × 2 = 115 (1)
Sr(2)−O(4) × 2 = 2.911(3)	O(3)−C−O(3) × 1 = 129 (2)
Sr(2)−O(5) × 4 = 2.527(9)	

(110)-sheared structure observed for the oxycarbonate $(Tl_{2/3}Cr_{1/3})Sr_4Cu_2(CO_3)O_7$ is generated by simply applying a shearing mechanism along *c*, in the (110) plane every five octahedra (Figure 4b). In both structures, the mixed carbonate/nitrate layers and the mixed carbonate/thallium/chromium layers, respectively, are flat. In contrast, the single intergrowth $(Tl_{5/6}Cr_{1/6})Sr_4Cu_2(CO_3)_{1/2}(NO_3)_{1/2}O_7$ exhibits flat $[CuO_2]_\infty$ layers, whereas the (110)-sheared oxycarbonate $(Tl_{2/3}Cr_{1/3})Sr_4Cu_2CO_3O_7$ is characterized by a waving of the $[CuO_2]_\infty$ layers. This undulation of the copper layers results from the ordered accommodation of the rows of carbonate groups and thallium rows within the same layer. The absence of superstructure reflections ($a \approx a_p$) for the oxycarbonitrate shows that the thallium species and CrO_4 tetrahedra are not distributed in an ordered way. These two compounds are also closely related to the thallium oxychromate $Tl_3(CrO_4)Sr_8Cu_4O_{16}$ (Figure 4c), which corresponds to an ordered substitution of one thallium row out of four by a row of CrO_4 tetrahedra in the "1201" structure. It is remarkable that the latter exhibits, like the oxycarbonate $(Tl_{2/3}Cr_{1/3})Sr_4Cu_2(CO_3)O_7$, a waving of the $[CuO_2]_\infty$ layers in order to allow an ordering phenomenon between the rows of CrO_4 groups and thallium rows.

The thallium oxychromate $Tl_3(CrO_4)Sr_8Cu_4O_{16}$ corresponds to a Cr/Tl ratio of $^1/_3$, higher than the one of the 1201-type parent of the oxycarbonitrate which corresponds to $[Tl_{5/6}Cr_{1/6}Sr_2CuO_5]$, i.e., Cr/Tl = $^1/_5$. The first one exhibits a superstructure which results from the Tl/Cr ordering within the $[Tl_{3/4}Cr_{1/4}O]$ intermediate layer whereas no long range ordering is observed within the $[Tl_{5/6}Cr_{1/6}O]$ layer. This suggests that the ordering mechanism is very sensitive to the chromium content and that small deviations from the average composition (issue to EDS analyses), namely $Tl_{5/6}Cr_{1/6}$, could involve local ordering features. One indeed observed from place to place, in the [001] HREM images, very small areas, a few nanometers wide, where the contrast is modulated along [100] or along [110]. One example is indicated in Figure 3b by small white arrows, where the local periodicity is $3a_p$, $3a_p$ and $2a_p$, respectively. Such short-range phenomena can be correlated to Tl/Cr orderings.

Besides these short-range orderings which attest of a local variation of the cationic distribution, very rare intergrowth defects are observed. An example is shown in Figure 5a (indicated by white arrowheads) where the carbonate/nitrate layers are imaged as bright rows. This defect results from the formation of the complex intergrowth of one 1201 member with two oxycarbonitrate slices, the corresponding idealized model is given in Figure 5b. It corresponds to the members $n = 2$ of the structural family obeying the formulation $[(Tl_{5/6}Cr_{1/6})Sr_2CuO_5][Sr_2Cu(CO_3)O_2]_n$.[3] In the present example, an additional feature is observed, which is a local shearing phenomenon. It implies that one carbonate layer is connected to one $[Tl_{5/6}Cr_{1/6}O]$ layer, according to a mechanism which is supposed to be that generating the sheared phases.

To understand the Tl/Cr ordering and the stabilization of the different phases of the system $Tl_{1-x}Cr_xSr_4Cu_2(CO_3)_{3x}(NO_3)_{1-3x+y}O_{7\pm\delta}$, samples exhibiting higher chromium contents ($x > ^1/_6$) were investigated. According to this thermal process, one always obtains multiphasic samples containing the oxycarbonate $(Tl_{2/3}Cr_{1/3})Sr_4Cu_2CO_3O_7$. The increase of the nitrate content favors the formation of mixtures of the "1201" cuprate $TlSr_2CuO_{5-\delta}$[11,12] and of the (110) sheared oxycarbonate $(Tl_{2/3}Cr_{1/3})Sr_4Cu_2CO_3O_7$. Such a behavior, observed for $0.1 < x < ^1/_3$ and $y \geq 0.75$, can be explained by a

(11) Kim, J. S.; Swinnea, J. S.; Steinfink, H. *J. Less Common Met.* **1989**, *156*, 347.
(12) Ohshima, E.; Kikuchi, M.; Izumi, F.; Hiraga, K.; Oku, T.; Nakajimo, S.; Ohnishi, N.; Morii, Y.; Funahashi, S.; Syono, Y. *Physica C* **1994**, *221*, 261.

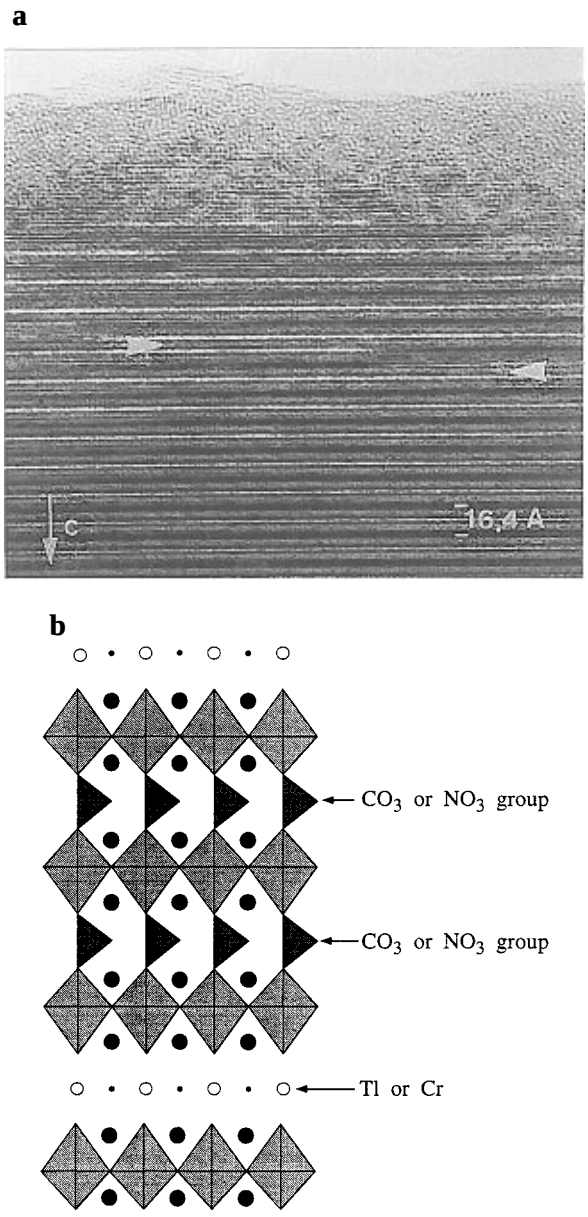

Figure 5. (a) [110] HREM image of a double carbonate-nitrate layer (indicated by a white arrowhead). A shearing mechanism involves the junction of one Tl/Cr layer with one carbonate/nitrate layer. (b) Idealized model of the defect.

decomposition of the nitrate groups, which then enhances the oxidization of the "1201" phase. But more important is the fact that, most of the time, both phases coexist within the same crystal, forming composite crystals. An example is given in the [110] image displayed in Figure 6a. The sheared structure domain is observed in the left part of the image (labeled S) and the "1201" domain in the right part. The carbonate rows are imaged as very bright segments, and the Tl/Cr layers as darker lines. The boundary is not planar; this feature can be explained considering that the $[CuO_2]_\infty$ layers and the $[SrO]_\infty$ layers are common to both structures and that the junction occurs only at the level of the mixed layers. This mechanism is periodically ensured in the sheared phase, and, as a consequence, the connection is very easily achieved and can take place at any level of the mixed (001) layers. This is shown in the idealized model in Figure 6b. The coherent junction of oxycarbonate- and 1201-type structures was previously observed in mercury based materials.[14,15]

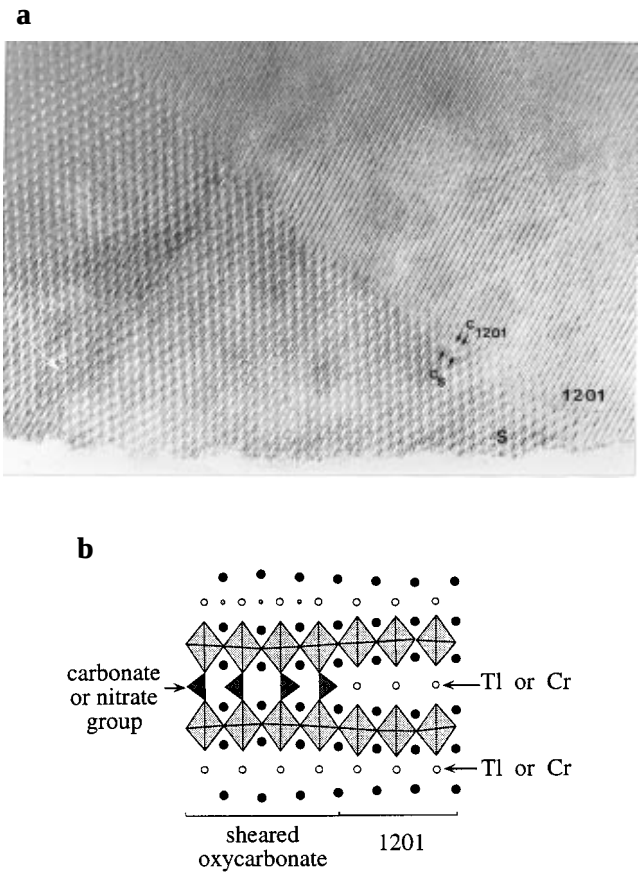

Figure 6. (a) HREM image showing the coexistence of the (110) sheared structure (labeled S) and the 1201 structure observed for high Cr content ($x > 1/6$). (b) Easy junction of the two structures.

The adaptability of the different frameworks is illustrated, in another way, by the formation of metastable phases, as observed in several crystallites where the sheared and nonsheared structures coexist. In such cases, the [110] ED patterns take on a typical appearance (Figure 7a). They result from the superimposition of two lattices which exhibit close parameters $b \approx ma_p\sqrt{2}$ and $c \approx 16.7$ Å but one is centered, a A-type lattice (index s), whereas the other is P-type (index m). The latter structure exhibits a c parameter which is slightly shorter than that of the (110) sheared structure, as seen from the elongated shape of the hhl reflections for high and even l values (which are common to both systems) and from the positions of the $(hhl)_m$ reflections for odd l_m values. The HREM image of the areas corresponding to the centered pattern exhibits the characteristic contrast of the (110) sheared structure as observed in the right part of Figure 7b (area labeled S). The carbonate rows appear as rows of bright dots and the contrast characteristic of the sheared structure with the alternation of bright and dark segments, five octahedra long, is clearly observed. For the second domain where the metastable phase is formed (area labeled M), the alternation of contrast arises only at the level of one mixed layer out of two. The $[SrO]_\infty$ and

(13) Huvé, M.; Michel, C.; Maignan, A.; Hervieu, M.; Martin, C.; Raveau, B. *Physica C* **1993**, *205*, 219.
(14) Pelloquin, D.; Hervieu, M.; Michel, C.; Maignan, A.; Raveau, B. *Physica C* **1994**, *227*, 215.
(15) Huvé, M.; Van Tendeloo, G.; Amelinckx, S.; Hervieu, M.; Raveau, B. *J. Solid State Chem.* **1995**, *120*, 332.

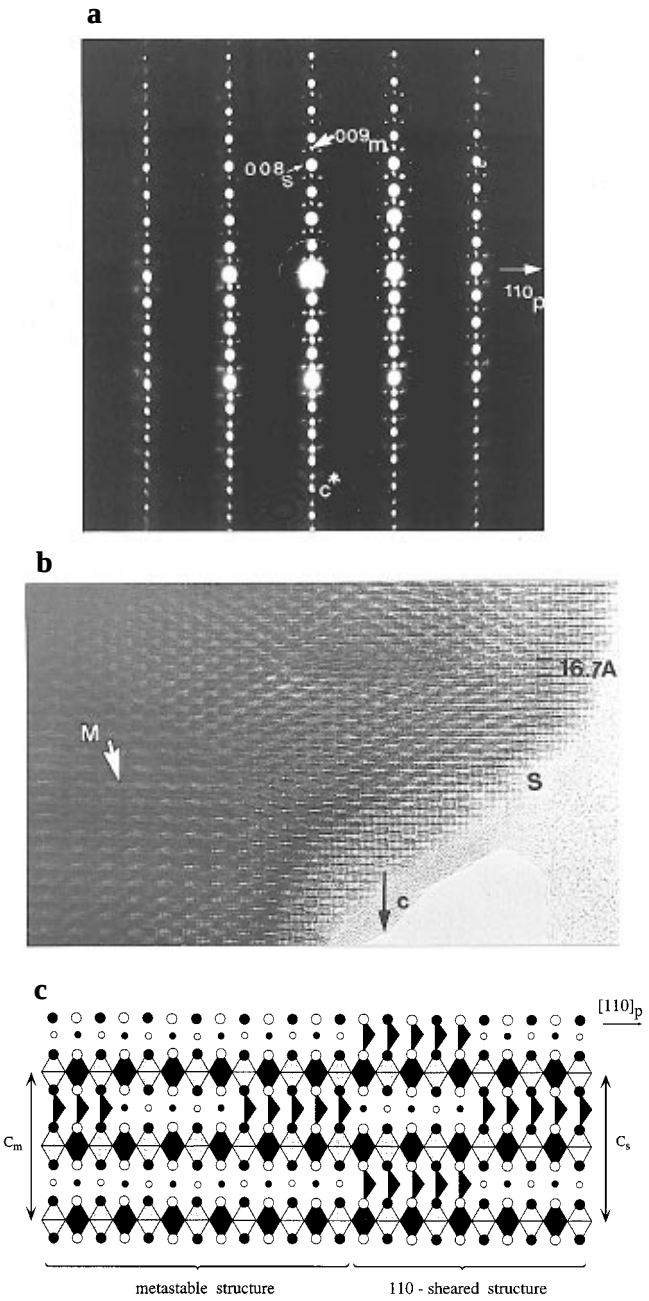

Figure 7. Example of formation of a metastable phase. (a) ED pattern showing the superposition of one P-type and one A-type variants. (b) HREM image: in the area where the metastable phase is formed (area labeled M and indicated by a white arrow), the carbonate−nitrate segments alternate with Tl/Cr segments in only one layer out of two. (c) Idealized drawing of the metastable structure.

$[CuO_2]_\infty$ layers are indeed unchanged and remain infinite through both structures and the difference lies in the nature of the intermediate layers stacked along the *c* axis. One pure [(Tl,Cr)O] layer (rows of dark dots) alternates with one mixed layer built from a sequence of six thallium atoms alternating with four carbonate (or nitrate) groups (rows of four bright dots and six dark dots). The metastable phase can therefore be described as built from the intergrowth of one 1201 member with one mixed oxycarbonate slice as shown in Figure 7c. It is interesting to note that the mixed layers are not arranged in a centered way, as observed in the sheared structures. This centered arrangement was assumed to be a way to decrease the strains due to the presence

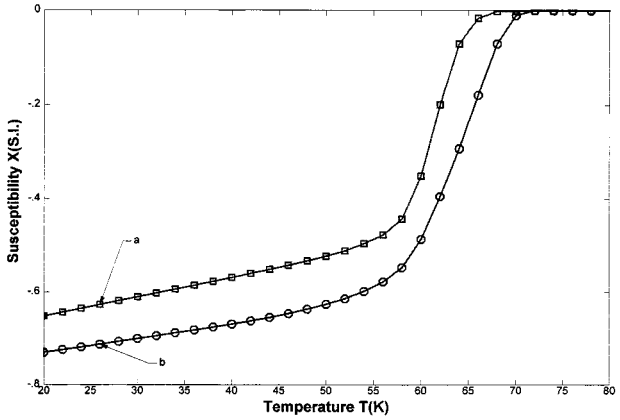

Figure 8. Susceptibility curves versus temperatures of the as-synthesized oxycarbonitrate $(Tl_{5/6}Cr_{1/6})Sr_4Cu_2(CO_3)_{1/2}(NO_3)_{1/2}O_7$ (curve a) and the annealed oxycarbonitrate $(Tl_{5/6}Cr_{1/6})Sr_4Cu_2(CO_3)_{1/2}(NO_3)_{1/2}O_7$ (curve b)

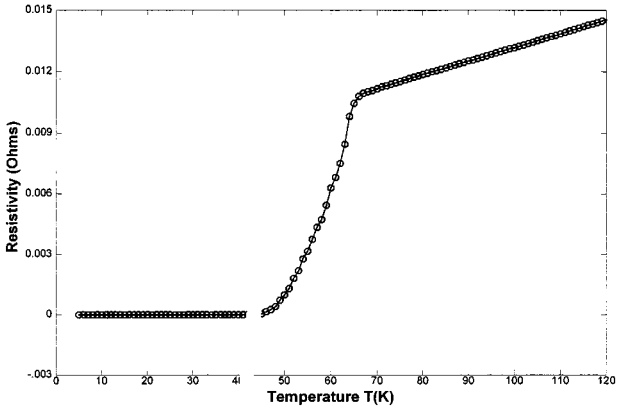

Figure 9. $R(T)$ curve showing a T_c (onset) of 65 K and a zero resistance at 48K.

of thallium and carbonate groups, which exhibit very different apical Tl−O and C−O bonds.[15] The fact that there is a thallium layer without carbonate, sandwiched between two perovskite slices, appears as sufficient to compensate the variations of the interatomic distances.

The susceptibility curves versus temperatures show that the as-synthesized oxycarbonitrate $(Tl_{5/6}Cr_{1/6})Sr_4Cu_2(CO_3)_{1/2}(NO_3)_{1/2}O_7$ exhibits a broader transition with a T_c (onset) of 65 K (Figure 8a). This broad transition is confirmed by the $R(T)$ curve (Figure 9) which shows a T_c (onset) of 65 K and a zero resistance at 48 K. Annealing under reducing atmospheres (Ar/H_2 at 280 °C) allow T_c to be increased to 68 K (Figure 8b). This superconducting behavior is similar to that of the (110)-sheared $(Tl_{2/3}Cr_{1/3})Sr_4Cu_2CO_3O_7$ (72 K as-synthesized and 77 K after reducing anneals[3]) and shows that the flatness of the $[CuO_2]_\infty$ layers, observed for the nonsheared phase $(Tl_{5/6}Cr_{1/6})Sr_4Cu_2(CO_3)_{1/2}(NO_3)_{1/2}O_7$, does not increase T_c with regard to the (110)-sheared oxycarbonate $(Tl_{2/3}Cr_{1/3})Sr_4Cu_2CO_3O_7$, which exhibits undulated $[CuO_2]_\infty$ layers.

Concluding Remarks

The possibility of introducing nitrate groups in the oxycarbonates derived from the "1201" structure has been evidenced for the first time. Such a substitution of NO_3^- anions for CO_3^{2-} leads to a new superconductor $(Tl_{5/6}Cr_{1/6})Sr_4Cu_2(CO_3)_{1/2}(NO_3)_{1/2}O_7$ whose chromium content is significantly smaller than that of the oxycarbon-

ate $(Tl_{2/3}Cr_{1/3})Sr_4Cu_2CO_3O_7$.[3] This decrease of the chromium content through nitrate substitution could be easily explained by the charge balance effect and supports the fact that these compounds are fully oxygenated "O_7", in agreement with the existence of Cr(VI). Such a behavior is in perfect agreement with the neutron diffraction results concerning the parent thallium oxychromate $Tl_3(CrO_4)Sr_8Cu_4O_{16}$, for which a fully oxygenated structure involving Cr(VI) has been evidenced.[7]

A transition from a (110)-sheared oxycarbonate $(Tl_{2/3}Cr_{1/3})Sr_4Cu_2CO_3O_7$ to a single (1201-S_2CC) intergrowth $Tl_{5/6}Cr_{1/6}Sr_4Cu_2(CO_3)_{1/2}(NO_3)_{1/2}O_7$ is observed as carbonate groups are partly replaced by nitrate groups. If one considers the similar geometry of the NO_3^- and CO_3^{2-} groups, such a transition cannot be due to this substitution but rather is due to the decrease of the chromium content in the structure. The presence of CrO_4 tetrahedra on the thallium sites of the "1201" structure, induces indeed a mismatch between the two sites "Tl" and "Cr", so that beyond a critical content of chromium a shearing may be introduced in the structure. Such a mismatch effect is comparable to that introduced by replacing strontium by barium: many pure "Sr_4" oxycarbonates are indeed single intergrowths,[13,14,16,17] whereas to date transitions to sheared oxycarbonates in the same system require mixed Ba/Sr layers.[15,18−20] Thus, this study shows again that the transition from nonsheared to sheared is mainly governed by a size effect within the rock salt layers either on the "Ba/Sr" sites or on the "Tl/M" sites.

It is also remarkable that the transition from the nonsheared to the sheared phase does not influence the *a* parameter of the tetragonal cell but leads to a large increase of the *c* parameter (16.41 to 16.67 Å). Such a variation is in contrast with the increase of the Cr(VI) content, whose size is smaller than that of Tl(III). Clearly, the shearing mechanism induces a mismatch between the wavy $[CuO_2]_\infty$ layers and the flat, mixed "Tl, Cr, C" layers that contributes to the increase of the *c* parameter.

The last important result deals with the fact that the substitution of nitrate groups does not influence the superconducting properties. This clearly shows that the geometrical factors and especially the planarity of the copper layers are not critical factors for superconductivity in these materials.

Acknowledgment. The authors are grateful to M. Daturi (Institute of Chemistry, University of GENOVA, Italy) for collection of infrared data and helpful discussion.

CM970370V

(16) Maignan, A.; Huvé, M.; Michel, C.; Hervieu, M.; Martin, C.; Raveau, B. *Physica C* **1993**, *208*, 149.
(17) Pelloquin, D.; Hervieu, M.; Malo, S.; Michel, C.; Raveau, B. *Physica C* **1995**, *246*, 1.
(18) Goutenoire, F.; Hervieu, M.; Maignan, A.; Michel, C.; Martin, C.; Raveau, B. *Physica C* **1993**, *210*, 359.
(19) Matsui, Y.; Ogawa, M.; Uehara, M.; Nakata, H.; Akimitsu, J. *Physica C* **1993**, *217*, 287.
(20) Uehara, M.; Sahoda, S.; Nakata, H.; Akimitsu, J.; Matsui, Y. *Physica C* **1994**, *222*, 27.